GEOLOGICAL SURVEY OF CANADA
OPEN FILE 7057

An outline of phase equilibrium

E. Froese

2013

Natural Resources Canada | Ressources naturelles Canada

Canada

GEOLOGICAL SURVEY OF CANADA
OPEN FILE 7057

An outline of phase equilibrium

E. Froese

2013

doi:10.4095/292552

This publication is available for free download through GEOSCAN (http://geoscan.ess.nrcan.gc.ca/).

Recommended citation
Froese, E., 2013. An outline of phase equilibrium; Geological Survey of Canada, Open File 7057, 12 p. doi:10.4095/292552

Publications in this series have not been edited; they are released as submitted by the author.

An outline of phase equilibrium

Edgar Froese
Geological Survey of Canada
edgarfroese@rogers.com

Abstract

A collection of systems of different composition defines a composition space which can be described by components defined as the minimum number of combinations of elements in fixed proportion required to express the composition of all phases in the considered systems. At stable equilibrium, and at constant pressure and temperature, each system is characterized by a minimum Gibbs energy $\mathbf{G}$. In the space defined by the components *n*, there exists a minimum $\mathbf{G}$ surface. If the compositional variation from system to system is continuous, the change of $\mathbf{G}$ along the minimum $\mathbf{G}$ surface can be described in differential form by

$$d\mathbf{G} = \sum \left(\frac{\partial \mathbf{G}}{\partial n_i} \right)_{P,T,\hat{n}_i} dn_i$$

where $\hat{n}_i$ refers to components other n_i. Designating the partial molar Gibbs energy of a component as $\bar{G}$, and integrating the expression gives

$$\mathbf{G} = \sum \bar{G}_i n_i$$

and division by $\sum n_i$ leads to

$$G = \sum \bar{G}_i X_i$$

where *G* is the molar Gibbs energy and *X* is the mole fraction of a component. A projection of the minimum molar *G* surface onto the composition base, in terms of *X*, results in a phase diagram.

Introduction

The first law of thermodynamics for a closed system (Denbigh, 1981), exchanging only pressure-volume work with the surroundings, is

$$d\mathbf{U} = dq - Pd\mathbf{V} \qquad (1)$$

where $\mathbf{U}$ is the total internal energy, *q* is the heat exchanged with the surroundings, *P* is the pressure, and $\mathbf{V}$ is the total volume.

The second law of thermodynamics implies, for changes in a closed system, the following relationship:

$$dq = Td\mathbf{S} - dq' \qquad (2)$$

where *T* is the absolute temperature, $\mathbf{S}$ is the total entropy, and *q'* is the uncompensated heat, which is zero for reversible changes and positive for irreversible changes (Prigogine and Defay, 1954). Substituting equation (2) into equation (1) gives

$$d\mathbf{U} + Pd\mathbf{V} - Td\mathbf{S} = -dq' \qquad (3)$$

and, at constant pressure and temperature,

$$d(\mathbf{U} + P\mathbf{V} - T\mathbf{S}) = -dq' \qquad (4)$$

Defining the expression in brackets as $\mathbf{G}$, the total Gibbs energy, leads to

$$d\mathbf{G} = -dq' \qquad (5)$$

Reaction equilibrium is concerned with the evaluation of *dq'* as a measure of irreversibility of a chemical reaction in a closed system whose composition is given by one side of the reaction equation; a summary is given by Froese (2006). Chemical reactions are written in terms of species; these are stoichiometric combinations of elements having a definite aggregate state or crystal structure. In order to evaluate *dq'* in terms of mole numbers of species, an additional postulate is introduced (Denbigh, 1981)

by assuming that the mole numbers of species can be treated as state variables and $d\mathbf{G}$ can be expressed by

$$d\mathbf{G} = \sum \left(\frac{\partial \mathbf{G}}{\partial n_i} \right)_{P,T,\hat{n}_i} dn_i = -dq' \quad (6)$$

where n_i is the number of moles of species *i* and $\hat{n}_i$ is the number of moles of all species other than *i*. A reaction equation relates the change of mole number of species n_i in such a way that

$$dn_i = \nu_i d\xi \quad (7)$$

where ν_i is the stoichiometric coefficient and ξ, as defined by equation (7), is the extent of reaction (Prigogine and Defay, 1954). Designating the partial derivative as the partial molar Gibbs energy of a species as $\bar{G}$ and substituting (7) into (6) leads to

$$d\mathbf{G} = \sum \bar{G}_i \nu_i d\xi = -dq' \quad (8)$$

Division by $d\xi$ gives

$$\left(\frac{\partial \mathbf{G}}{\partial \xi} \right)_{P,T} = \sum \nu_i \bar{G}_i = -\frac{dq'}{d\xi} \quad (9)$$

A reaction will tend to decrease $\mathbf{G}$ until $\mathbf{G}$ reaches a minimum value at stable equilibrium.

In contrast to reaction equilibrium, phase equilibrium is concerned with various closed systems of different composition, each at stable equilibrium. The composition of the various systems can be represented in composition space which can be defined in terms of components; these are the minimum number of element combinations in a fixed ratio required to express the composition of all phases in all considered systems. Although each system has reached minimum $\mathbf{G}$, in a comparison of different systems, there is a change in $\mathbf{G}$. In order to express such variation in $\mathbf{G}$ from system to system in differential form, the closed systems in composition space must be regarded as forming a continuum. The systems of different composition define a minimum $\mathbf{G}$ surface in composition space, which is expressed in terms of components; The minimum $\mathbf{G}$ surface is a function of the components and, therefore, the variation of $\mathbf{G}$ from system to system along the minimum $\mathbf{G}$ surface is given by

$$d\mathbf{G} = \sum \left(\frac{\partial \mathbf{G}}{\partial n_i} \right)_{P,T,\hat{n}_i} dn_i \quad (10)$$

where n_i is the number of moles of component *i* and $\hat{n}_i$ is the number of moles of all components other than *i*. This is essentially equation 92 in Gibbs (1876). It looks similar to equation (6) but, in this case, there is no inequality and $d\mathbf{G}$ is not equal to *-dq'*. And, very importantly, the *n*'s refer to components rather than species. This distinction, in many cases, has to be inferred from the context but Anderson (2005) has made it explicitly. The partial derivative in equation (10) is the partial molar Gibbs energy $\bar{G}$ of a component. Thus

$$d\mathbf{G} = \sum \bar{G}_i dn_i \quad (11)$$

This equation can be integrated if, during integration, the $\bar{G}_i$'s are kept constant by keeping the ratios between the n_i's constant (Denbigh, 1981), resulting in

$$\mathbf{G} = \sum \bar{G}_i n_i \quad (12)$$

Division by $\sum n_i$ gives

$$G = \sum \bar{G}_i X_i \quad (13)$$

where *G* is the molar Gibbs energy of a system in composition space and X is the mole fraction of a component.

These concepts are illustrated in Fig. 1a, where the molar *G* of forsterite and enstatite, taken from Berman (1988), are plotted against the composition $MgO - SiO_2$. Also shown is *G* of a mixture of 0.5 moles of periclase (MgO) and 0.5 moles of quartz (SiO_2). Reaction equilibrium would be concerned with changes in total $\mathbf{G}$ of a system of composition $0.5\ MgO \cdot SiO_2$ represented by the reaction

$$0.5\ MgO\ (\text{periclase}) + 0.5\ SiO_2\ (\text{quartz}) = 0.5\ MgSiO_3\ (\text{enstatite}) \quad (14)$$

According to equation (9), the system will tend to vary ξ until a minimum $\mathbf{G}$ is reached, which will be when periclase and quartz have been converted to enstatite. The system has been chosen to be of such composition that the total Gibbs energy $\mathbf{G}$ is equal to the molar Gibbs energy *G*, so that it can be shown in Fig. 1.

By way of contrast, phase equilibrium considers the *G* changes along the straight line connecting forsterite and enstatite. The line represents a continuum of closed systems, each at minimum *G* according to equation (13); the value of *G* of any system along this line is given by

$$G = \bar{G}_{MgO} X_{MgO} + \bar{G}_{SiO_2} X_{SiO_2} \quad (15)$$

and the values of $\bar{G}_{MgO}$ and $\bar{G}_{SiO_2}$ are given by the intercepts at the ends of the composition scale. If this line is projected onto the composition base, a phase diagram is obtained.

Composition space

The composition space in which one wishes to examine a collection of closed systems depends on the composition of phases to be considered. The minimum number of compositional variables required to express the composition of all species in all phases in all systems is usually obvious if the species consist of few elements. In dealing with more complex species, it is better to follow a procedure suggested by Smith and Missen (1982) and used e.g. by Gordon (1991) involving the construction of a formula matrix. The columns consist of the composition of species and the rows are formed by elements. An example is given in Table 1.

Table 1. An example of a formula matrix.

	quartz	sillimanite	K feldspar	steam	almandine	pyrope	annite	phlogopite	Fe cordierite	cordierite
	SiO_2	Al_2SiO_5	$KAlSi_3O_8$	H_2O	$Fe_3Al_2Si_3O_{12}$	$Mg_3Al_2Si_3O_{12}$	$KFe_3Si_3AlO_{10}(OH)_2$	$KMg_3Si_3AlO_{10}(OH)_2$	$Fe_2Al_4Si_5O_{18}$	$Mg_2Al_4Si_5O_{18}$
Si	1	1	3	0	3	3	3	3	5	5
Al	0	2	1	0	2	2	1	1	4	4
Fe	0	0	0	0	3	0	3	0	2	0
Mg	0	0	0	0	0	3	0	3	0	2
K	0	0	1	0	0	0	1	1	0	0
H	0	0	0	2	0	0	2	2	0	0
O	2	5	8	1	12	12	12	12	18	18

The composition space required to represent these species is given by the space spanned by the columns. This space is adequately specified by giving a minimum number of vectors (basis vectors) that span this space. This number is given by the rank; in this example, it is 6. Any six vectors could be chosen, i.e. any six combination of elements with a fixed ratio; these are the components. They have no attributes of aggregate state or crystal structure; they convey only an information of composition. On the minimum $\mathbf{G}$ surface of a continuum of systems in a multi-component composition space, components and combinations of components have defined values of $\mathbf{G}$ and thus any mass balance is also a $\mathbf{G}$ energy balance.

Systems in multi-component space

Graphical representation in the form of phase diagrams presents difficulties if the collection of closed systems to be considered requires a multi-component space. Phase diagrams are limited to three, or, at the most, four components. Some relief from this restriction is provided by Korzhinskii's (1959) suggestion that $\bar{G}_i$, the partial molar Gibbs energy of a component, rather than the mole number n_i of a component, can be used as an independent variable. Thus, it is convenient to recognize two groups of components. In the first group (*j*-components), the *n*'s are chosen as independent variables and, in the second group (*k*-components), the $\bar{G}_i$'s. This designation, taken from Thompson (1970), catches the essence of his distinction but he, in addition, discussed geological reasons for making such choice. Thus equation (12) can be written as two sums:

$$\mathbf{G} = \sum \bar{G}_j n_j + \sum \bar{G}_k n_k \qquad (16)$$

or

$$(\mathbf{G} - \sum \bar{G}_k n_k) = \sum \bar{G}_j n_j \qquad (17)$$

The left side of equation (17) is a function derived by Korzhinskii (1959) and designated as $\mathbf{G}_0$. Thompson (1970) used the letter $\mathbf{L}$, which is better established in the geological literature and is used here. Since $\mathbf{G}$ is at a minimum, if all $\bar{G}_k$'s are kept constant, $\mathbf{L}$ also has a minimum value and is equal to

$$\mathbf{L} = \sum \bar{G}_j n_j \qquad (18)$$

Division by $\sum n_j$ gives

$$L = \sum \bar{G}_j X_j \qquad (19)$$

where *L* is the molar value of the $\mathbf{L}$ function and *X* is the mole fraction of a component.

Considering the composition space MgO –SiO_2, if n_{MgO} and $\bar{G}_{SiO_2}$ are chosen as independent variables, MgO is a *j*-component and SiO_2 is a *k*-component (Fig. 1b). If a line is drawn through the molar Gibbs energy *G* of enstatite and the chosen value of $\bar{G}_{SiO_2}$, the molar Gibbs energy of enstatite can be expressed as

$$0.5G_{MgSiO_3} = \bar{G}^*_{MgO}(0.5) + \bar{G}_{SiO_2}(0.5) \qquad (20)$$

and the intercept on the MgO axis in a system containing enstatite at the imposed value of $\bar{G}_{SiO_2}$ is given by

$$\bar{G}^*_{MgO} = G_{MgSiO_3} - \bar{G}_{SiO_2} \qquad (21)$$

The star here is used to indicate that MgO is the only *j*-component in the composition space and, therefore, $\bar{G}^*_{MgO}$ is equal to L. A projection of $\bar{G}^*_{MgO}$ onto the composition axis MgO – SiO_2 results in a one-dimensional phase diagram (Fig. 1b). If a line is drawn from $\bar{G}_{SiO_2}$ through forsterite, the intercept on the MgO axis gives $\bar{G}^*_{MgO}$ in a system containing forsterite at the imposed value of $\bar{G}_{SiO_2}$. This $\bar{G}^*_{MgO}$ value is more positive than in the case of enstatite and, therefore, forsterite does not appear on the phase diagram.

The outlined approach is, of course, particularly useful for systems in a multi-component composition space. In the example given in Table 1, the components could be grouped as follows:
j-components: FeO, MgO
k-components: SiO_2, Al_2SiO_5, $KAlSi_3O_8$, H_2O
Values of molar Gibbs energies of species, taken from Berman's database June92.GSC, are given in Table 2. They imply a particular choice of energy datum, as given by Berman (1988).

Table 2. Thermodynamic data at 700°C and 4 kb

Species	Formula	G J mol^{-1}	$\bar{G}^*_{FeO}$ J mol^{-1}	$\bar{G}^*_{FeO}$ J mol^{-1} + 359 156	$\bar{G}^*_{MgO}$ J mol^{-1}	$\bar{G}^*_{MgO}$ J mol^{-1} + 683 155
quartz	SiO_2	-968 891				
sillimanite	Al_2SiO_5	-2 733 074				
K feldspar	$KAlSi_3O_8$	-4 257 530				
steam	H_2O	-378 112				
almandine	$Fe_3Al_2Si_3O_{12}$	-5 748 323	- 359 156	0		
pyrope	$Mg_3Al_2Si_3O_{12}$	-6 690 443			-673 196	9 954
annite	$KFe_3Si_3AlO_{10}(OH)_2$	-5 705 508	- 356 622	2 534		
phlogopite	$KMg_3Si_3AlO_{10}(OH)_2$	-6 681 090			-681 816	1 334
Fe cordierite	$Fe_2Al_4Si_5O_{18}$	-9 082 456	-354 818	4 338		
cordierite	$Mg_2Al_4Si_5O_{18}$	-9 739 121			-683 150	0

For species listed in Table 2, the value of either $\bar{G}^*_{FeO}$ or $\bar{G}^*_{MgO}$ can be obtained by subtracting appropriate amounts of the *k*-components, following the pattern of equation (21) but involving more than one *k*-component. This is done in Table 3, using the following $\bar{G}$ values of the *k*-components:

$\bar{G}_{SiO_2}$ = G of quartz

$\bar{G}_{Al_2SiO_5}$ = G of sillimanite

$\bar{G}_{KAlSi_3O_8}$ = G of K feldspar

$\bar{G}_{H_2O}$ = G of steam

Table 3. $\bar{G}^*_{FeO}$ and $\bar{G}^*_{MgO}$ values of species at specified $\bar{G}$'s of *k*-components

almandine	$Fe_3Al_2Si_3O_{12}$	$\bar{G}^*_{FeO} = \frac{1}{3} G_{Fe_3Al_2Si_3O_{12}} - \frac{1}{3}\bar{G}_{Al_2SiO_5} - \frac{2}{3}\bar{G}_{SiO_2}$
pyrope	$Mg_3Al_2Si_3O_{12}$	$\bar{G}^*_{MgO} = \frac{1}{3} G_{Mg_3Al_2Si_3O_{12}} - \frac{1}{3}\bar{G}_{Al_2SiO_5} - \frac{2}{3}\bar{G}_{SiO_2}$
annite	$KFe_3Si_3AlO_{10}(OH)_2$	$\bar{G}^*_{FeO} = \frac{1}{3} G_{KFe_3Si_3AlO_{10}(OH)_2} - \frac{1}{3}\bar{G}_{KAlSi_3O_8} - \frac{1}{3}\bar{G}_{H_2O}$
phlogopite	$KMg_3Si_3AlO_{10}(OH)_2$	$\bar{G}^*_{MgO} = \frac{1}{3} G_{KMg_3Si_3AlO_{10}(OH)_2} - \frac{1}{3}\bar{G}_{KAlSi_3O_8} - \frac{1}{3}\bar{G}_{H_2O}$
Fe cordierite	$Fe_2Al_4Si_5O_{18}$	$\bar{G}^*_{FeO} = \frac{1}{2} G_{Fe_2Al_4Si_5O_{18}} - \bar{G}_{Al_2SiO_5} - \frac{3}{2}\bar{G}_{SiO_2}$
cordierite	$Mg_2Al_4Si_5O_{18}$	$\bar{G}^*_{MgO} = \frac{1}{2} G_{Mg_2Al_4Si_5O_{18}} - \bar{G}_{Al_2SiO_5} - \frac{3}{2}\bar{G}_{SiO_2}$

The values of $\bar{G}^*_{FeO}$ and $\bar{G}^*_{MgO}$ of species listed in Table 2 can be plotted on a diagram of $\sum \bar{G}_j X_j$ against the composition axis FeO - MgO (Fig. 2). The large difference between the $\bar{G}^*_{FeO}$ values and the $\bar{G}^*_{MgO}$ values of Fe and Mg species causes difficulties in plotting. Since $\bar{G}^*_{FeO}$ and $\bar{G}^*_{MgO}$ bear no relation to each other, the origin of the energy axes can be shifted arbitrarily. To achieve a more readable plot, $\bar{G}^*_{FeO}$ of $Fe_3Al_2Si_3O_{12}$ and $\bar{G}^*_{MgO}$ of $Mg_2Al_4Si_5O_{18}$ have been set to 0. If almandine and pyrope were the only species considered and did not form a solid solution, $\sum \bar{G}_j X_j$ of a system including both would be given by

$$\sum \bar{G}_j X_j = \bar{G}^*_{FeO} X_{FeO} + \bar{G}^*_{MgO} X_{MgO} \qquad (22)$$

and, assuming an ideal solution of components FeO and MgO,

$$\sum \bar{G}_j X_j = (\bar{G}^*_{FeO} + RT \ln X_{FeO}) X_{FeO} + (\bar{G}^*_{MgO} + RT \ln X_{MgO}) X_{MgO} \qquad (23)$$

For instance, in a system of composition of X_{MgO} = 0.3, $\sum \bar{G}_j X_j$ = - 1956 J mol^{-1}. The values of $\sum \bar{G}_j X_j$ can be shown as a curve (Fig. 2). Similar curves can be calculated for biotite and cordierite. If garnet, biotite, and cordierite are considered in the same composition space, the minimum $\sum \bar{G}_j X_j$ line is given by curved lines of the solid solutions connected by straight-line segments formed by common tangents. A phase diagram is obtained by projecting the minimum $\sum \bar{G}_j X_j$ line onto the composition axis (Fig. 2). The phase diagram calculated with the program Theriak/Domino (de Capitani and Petrakakis, 2010) gives the following compositions in terms of X_{MgO}: garnet = 0.124, biotite = 0.359 and 0.526, cordierite = 0.621.

A tangent at any point of the minimum $\sum \bar{G}_j X_j$ line has intercepts $\bar{G}_{FeO}$ and $\bar{G}_{MgO}$ on the FeO and MgO axes. The variation of $\bar{G}_{FeO}$ with composition is shown in Figure 3. A different shift of the origin of the energy axes would not change the phase diagram but the intercepts $\bar{G}_{FeO}$ and $\bar{G}_{MgO}$ on the FeO and MgO axes would have different values.

Ternary phase diagrams

Because biotite and orthopyroxene contain an appreciable amount of aluminum, a more realistic grouping of components is as follows:

j-components: Al_2O_3, FeO, MgO

k-components: SiO_2, $KAlSi_3O_8$, H_2O

The minimum $\sum \bar{G}_j X_j$ values of systems with varying amounts of *j*-components can be calculated and plotted against a triangular base of Al_2O_3 –FeO – MgO; they form a surface in space. This minimum $\sum \bar{G}_j X_j$ surface can be projected onto the composition base producing a ternary phase diagram (Fig. 4); this diagram, showing biotite and orthopyroxene as ternary solutions, has been calculated using the program Theriak/Domino (de Capitani and Petrakakis, 2010). The database used was that of Holland and Powell (1998) incorporating nonideal solution models. In metamorphic petrology, it is common practice to include the total amount of Al_2O_3 of a composition to be plotted and subtract enough Al_2O_3 required to combine with other oxides to form *k*-components. Thus, in Figure 4, the top corner would be labelled $Al_2O_3 – K_2O$.

A tangent plane at any point of the minimum $\sum \bar{G}_j X_j$ surface will form intercepts on the axes of the three *j*-components; these give the $\bar{G}$ values of Al_2O_3, FeO, and MgO, which can be shown as contours on the ternary phase diagram. In Fig. 4, a contour each of $\bar{G}_{FeO}$ and $\bar{G}_{MgO}$ is shown diagrammatically. Such a contour is a curved line in a one-phase field. It is not defined if there is a fixed

ratio of some *j*-components in the phase; e.g., in cordierite, Al_2O_3 is equal to (FeO + MgO). The contour coincides with a tie line in two-phase fields and is absent in three-phase fields; see also Figure 43 in Korzhinskii (1959).

Phase rule

A continuum of thermodynamic systems has $c + 2$ independent variables, where c is the number of components and 2 stands for pressure and temperature. The choice of either n or $\bar{G}$ as the independent variable of a component is subject to some restrictions. Equation (11) has been integrated by assuming that $\mathbf{G}$ is a function of the mole number of components and that the partial molar Gibbs energies of components are kept constant. This is achieved by keeping the ratios of the components constant and from the additional knowledge that intensive properties like $\bar{G}$ are affected only by the relative amounts and not by the absolute amounts of components (Denbigh, 1981). If the resulting equation (12) is differentiated again, and allowing the $\bar{G}_i$s to vary, the following relationship is obtained:

$$d\mathbf{G} = \sum \bar{G}_i dn_i + \sum n_i d\bar{G}_i \quad (23)$$

In view of the validity of equation (11), it follows that

$$\sum n_i d\bar{G}_i = 0 \quad (24)$$

which is the Gibbs-Duhem equation, essentially the same as equation 97 in Gibbs (1876). The Gibbs-Duhem equation gives a different relationship of the $\bar{G}$'s for each phase. Therefore, for each system, the number of independent n's chosen must be equal at least to the number of phases p. Since the total number of independent variables is equal to $c + 2$, the maximum number of independent intensive variables P, T, and $\bar{G}$'s, designated by the variance f, is given by the phase rule

$$f = c + 2 - p \quad (25)$$

In the diagram shown in Fig. 4, there are three extensive variables corresponding to the *j*-components. The mole numbers can be given by specifying $\sum n_j = 1$ and giving two mole fractions which are numerically equal to mole numbers. There are three *k*-components. Thus, the total number of components is 6 and

$$f = 8 - p \quad (26)$$

Since P, T, and $\bar{G}$'s of the three *k*-components have been chosen as independent intensive variables for the diagram as a whole, the option for choosing additional intensive variables is reduced to

$$f = 3 - p \quad (27)$$

In Figure 4, the $\bar{G}$'s of the *j*-components can be shown as contours in their dependence on the X_j's.

In order to define any system within the compositional variation given by the *j*-components, there are several options. In one-phase fields, either two mole fractions, or the $\bar{G}$'s of two *j*-components, or one mole fraction and $\bar{G}$ of one *j*-component can be chosen. In two-phase field, either one mole fraction or $\bar{G}$ of one *j*-component in one phase can be chosen. And in three-phase fields, the choice is limited to two mole fractions.

Univariant curves around an invariant point

The phase diagram of Figure 4 includes some three-phase assemblages; these are stable over a field on a pressure-temperature diagram and, accordingly, are designated as bivariant. Assemblages of four phases in a system with three *j*-components are univariant, i.e., they are stable along a curve on a pressure-temperature diagram. At any one point along the univariant line, there is a bulk composition, in terms of *j*-components, that can be expressed by two alternate configurations of the phase assemblage, as illustrated by Gibbs (1876):

1. The composition of one phase falls inside a triangle formed by the compositions of the other three phases.

2. The compositions of the four phases form a quadrilateral and a particular bulk composition can be expressed by a combination of two opposite diagonal phases.

This composition equivalence is expressed graphically by the appearance (or disappearance) of a phase or by an exchange of tie lines. A mass balance can be written in terms of the composition of phases and the composition of *k*-components. For instance, at a point of the univariant curve representing the univariant assemblage biotite-sillimanite-garnet–cordierite, one could write

biotite + sillimanite + SiO_2 = garnet + cordierite + $KAlSi_3O_8$ + H_2O

Such mass-balance equation is commonly also called a reaction but it differs from reactions encountered in the study of reaction equilibrium which are written in terms of the composition of species with fixed stoichiometric coefficients. It may be more appropriately called a compatibility equation. The numerical coefficients of the phases and of the *k*-components change along the univariant curve. Such change can lead to a sign reversal of the numerical coefficient of a reactant or product creating a singular point (Abart et al., 1992), where the reactant or product disappears from the equation.

Univariant curves will intersect in an invariant point. The example shown in Figure 5 has been calculated with the program Theriak/Domino (de Capitani and Petrakakis, 2010) and using the database of Holland and Powell, 1998). The intersection of pressure-temperature curves and their position are entirely determined by the change of the partial molar Gibbs energy of all components with pressure and temperature. Such regularity has been summarized in the form of Schreinemakers' rules (Zen, 1966). Lindsley et al. (1968) suggested the following convenient procedure to check the consistency of the arrangement of univariant curves around an invariant point. The compatibility equation is written onto the univariant curve, with reactants and products on opposite sides of the curve. A univariant curve is labelled with the phase not involved in the compatibility equation. If the univariant curve is extended metastably into the sector across the invariant point, the labelled phase must be present in the two halves of the two compatibility equations in the sector. Thus the metastable extension of univariant curve (biotite) falls into the sector on the left of Figure 5 with compatibilities (biotite + garnet) and (biotite + sillimanite) .

Acknowledgments

I am much obliged to R.G. Berman for guidance in the use of Theriak/Domino. An earlier version of this paper was critically read by G.M. Anderson and T.M. Gordon. The present paper was reviewed by T.M. Gordon which led to further discussions. The diagrams were drafted by S. Davis and K. Nguyen.

References

Abart, R., Connolly, J.A.D. and Trommsdorff, V.
1992: Singular point analysis: construction of Schreinemakers projections for systems with a binary solution; American Journal of Science, v. 292, p. 778-805.

Anderson, G. M.
2005: Thermodynamics of natural systems; Cambridge University Press, Cambridge, 648 p.

Berman, R.G.
1988: Internally-consistent thermodynamic data for minerals in the system Na_2O-K_2O-CaO-MgO-FeO-Fe_2O_3-Al_2O_3-SiO_2-TiO_2-H_2O-CO_2; Journal of Petrology, v. 29, p. 445-552.

de Capitani, C. and Petrakakis, K.
2010: The composition of equilibrium assemblage diagrams with Theriak/Domino software; American Mineralogist, v. 95, p. 1006-1016

Denbigh, K.
1981: The principles of chemical equilibrium; Cambridge University Press, Cambridge, United Kingdom, 494 p, (fourth edition)

Froese, E.
2006: An outline of reaction equilibrium; Geological Survey of Canada, Current Research 2006-H2, 12 p.

Gibbs, J.W.
1876: On the equilibrium of heterogeneous substances; Transactions of the Connecticut Academy, v. 3, p. 108-248.

Gordon, T. M.
1992: Generalized thermobarometry: solution of the inverse chemical equilibrium problem using data for individual species; Geochimica et Cosmochimica Acta, v. 56, p. 1793-1800.

Holland T.J.B. and Powell, R.
1998: An internally consistent thermodynamic data set for phases of petrological interest; Journal of Metamorphic Geology, v.16, p, 309-343.

Korzhinskii, D. S.
1959: Physicochemical basis of the analysis of the paragenesis of minerals; Consultants Bureau, Inc., New York, 142 p.

Lindsley, D.H., Speidel, D.H. and Nafzinger, R.H.
1968: P-T- f_{O_2} relations in the system Fe-O-SiO_2; American Journal of Science, v. 266, p. 342-360.

Prigogine, I. and Defay, R.
1954: Chemical thermodynamics; Longmans, Green and Company, London. United Kingdom, 543 p.

Smith, W.R. and Missen, R.W.
1982: Chemical reaction equilibrium analysis: theory and algorithms; John Wiley and Sons, New York.

Thompson, J. B.
1970: Geochemical reaction and open systems; Geochimica et Cosmochimica Acta, v. 34, p. 529-551.

Zen E-an
1966: Construction of pressure-temperature diagrams for multi-component systems after the method of Schreinemakers – a geometric approach;
United States Geological Survey, Bulletin 1225, 56 p.

Figures

Fig. 1. Phase relations in the composition space $MgO - SiO_2$.
   a) with MgO and SiO_2 as *j*-components
   b) with MgO as *j*-component and SiO_2 as *k*-component.

Fig. 2. Phase relations in the composition space $FeO - MgO - SiO_2 - Al_2SiO_5 - KAlSi_3O_8 - H_2O$ with FeO and MgO as *j*-components and SiO_2, Al_2SiO_5, $KAlSi_3O_8$, and H_2O as *k*-components.

Fig. 3. The variation of $\bar{G}_{FeO}$ in the composition space $FeO - MgO - SiO_2 - Al_2SiO_5 - KAlSi_3O_8 - H_2O$ with FeO and MgO as *j*-components and SiO_2, Al_2SiO_5, $KAlSi_3O_8$, and H_2O as *k*-components.

Fig. 4. Phase relations the composition space $Al_2O_3 - FeO - MgO - SiO_2 - KAlSi_3O_8 - H_2O$ with Al_2O_3, FeO, and MgO as *j*-components and SiO_2, $KAlSi_3O_8$, and H_2O as *k*- components.

Fig. 5. Univariant curves around the invariant point biotite-sillimanite-garnet-cordierite-orthopyroxene in the composition space $Al_2O_3 - FeO - MgO - SiO_2 - KAlSi_3O_8 - H_2O$ with Al_2O_3, FeO, and MgO as *j*-components and SiO_2, $KAlSi_3O_8$, and H_2O as *k*- components.

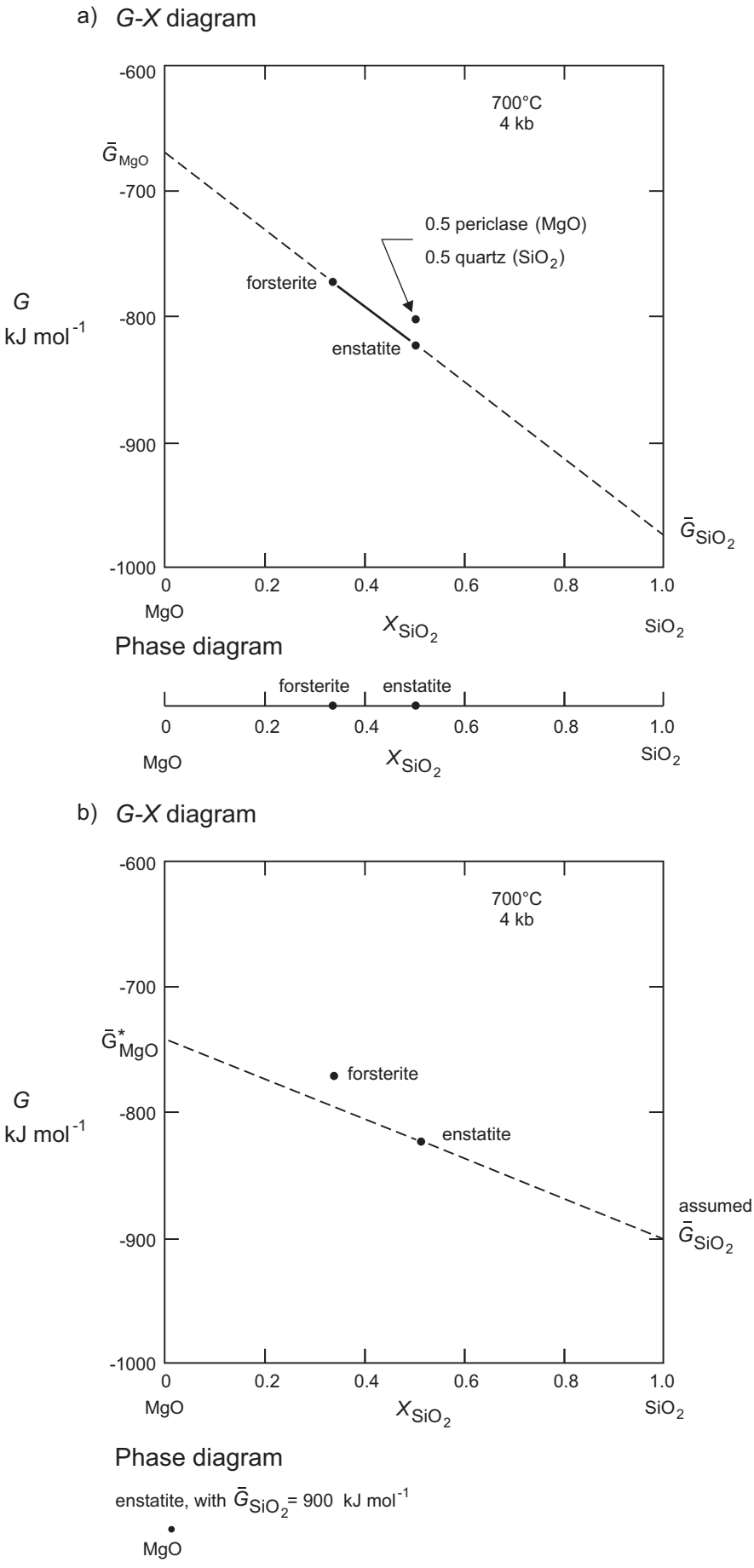

Figure 1. Phase relations in the composition space MgO – SiO_2.
a) with MgO and SiO_2 as *j*-components
b) with MgO as *j*-component and SiO_2 as *k*-component.

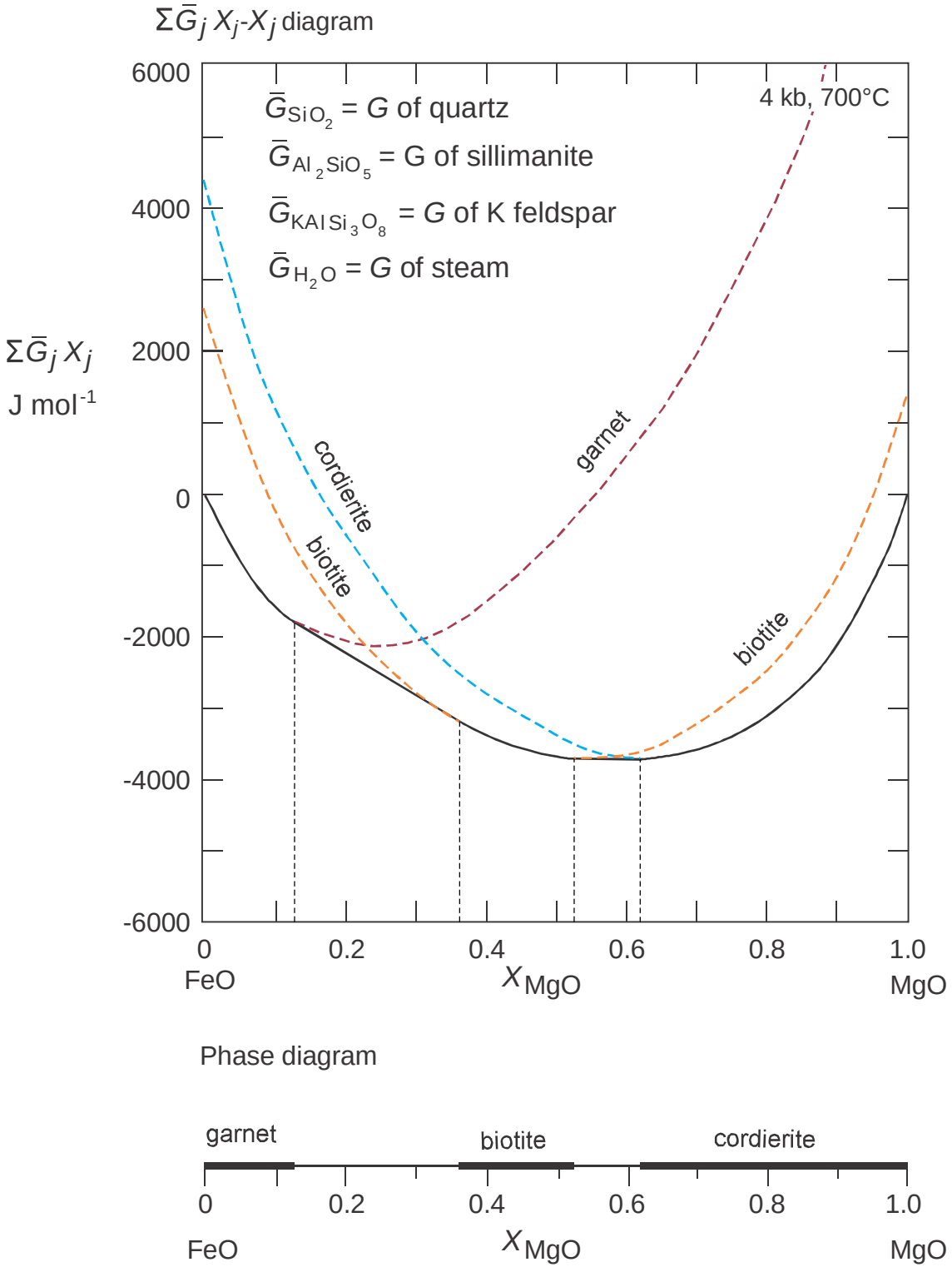

Figure 2. Phase relations in the composition space FeO - MgO - SiO_2 - Al_2SiO_5 - $KAlSi_3O_8$ - H_2O with FeO and MgO as *j*-components and SiO_2, Al_2SiO_5, $KAlSi_3O_8$, and H_2O as *k*-components.

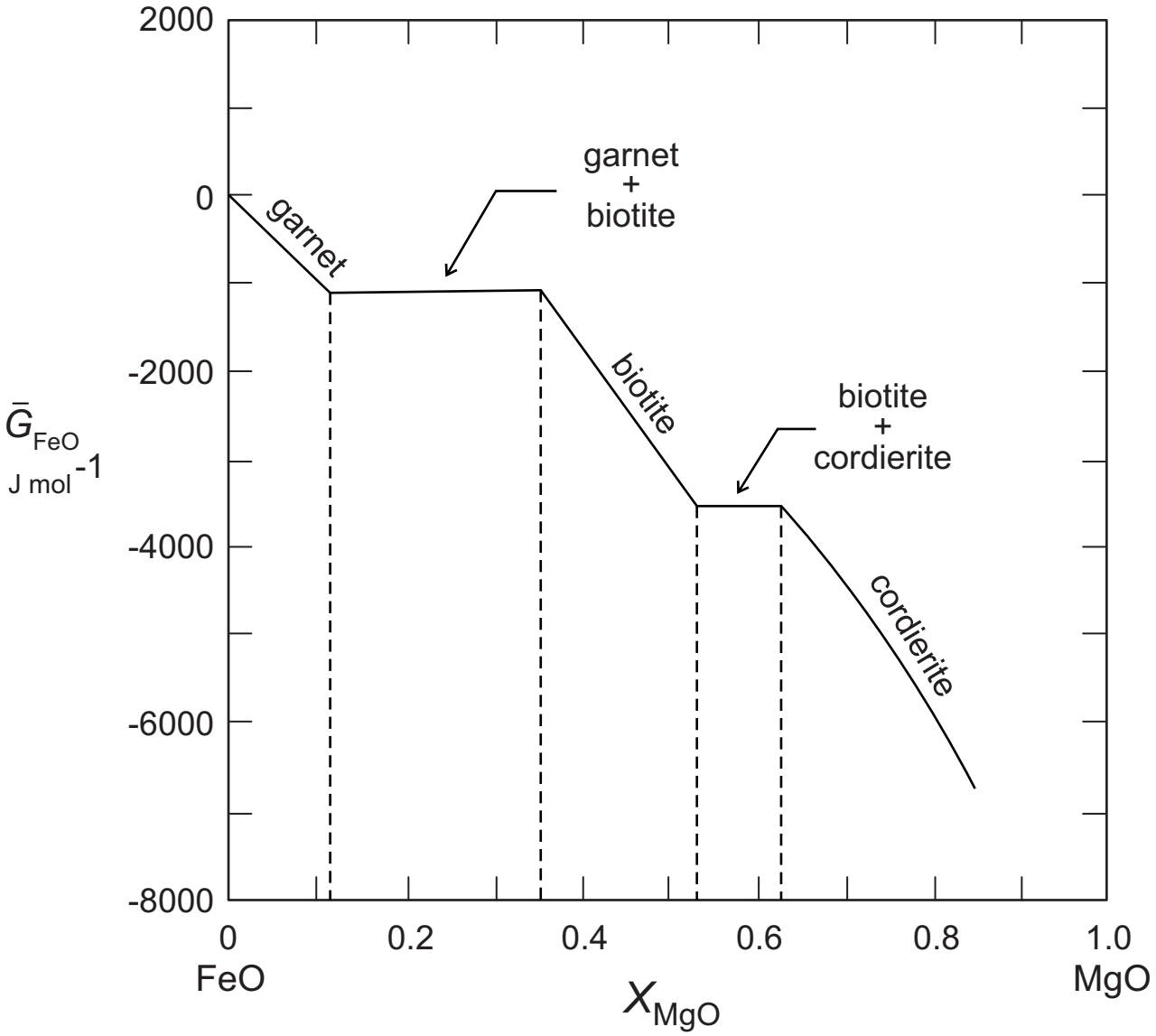

Figure 3. The variation of G_{FeO} in the composition space FeO - MgO - SiO_2 - Al_2SiO_5 - $KAlSi_3O_8$ - H_2O with FeO and MgO as *j*-components and SiO_2, Al_2SiO_5, $KAlSi_3O_8$, and H_2O as *k*-components.

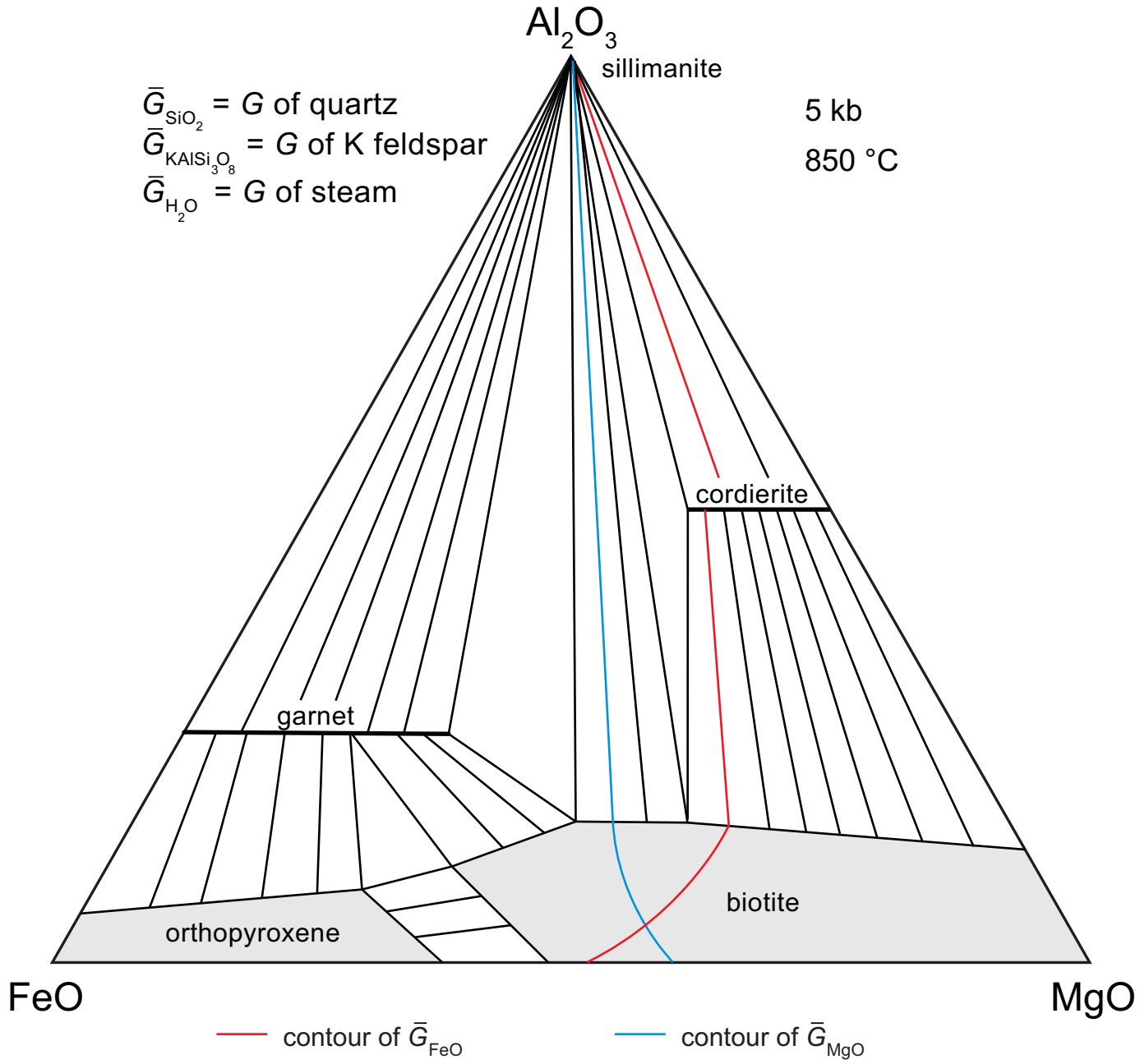

Figure 4. Phase relations the composition space Al_2O_3 - FeO - MgO - SiO_2 - $KAlSi_3O_8$ - H_2O with Al_2O_3, FeO, and MgO as *j*-components and SiO_2, $KAlSi_3O_8$, and H_2O as *k*-components.

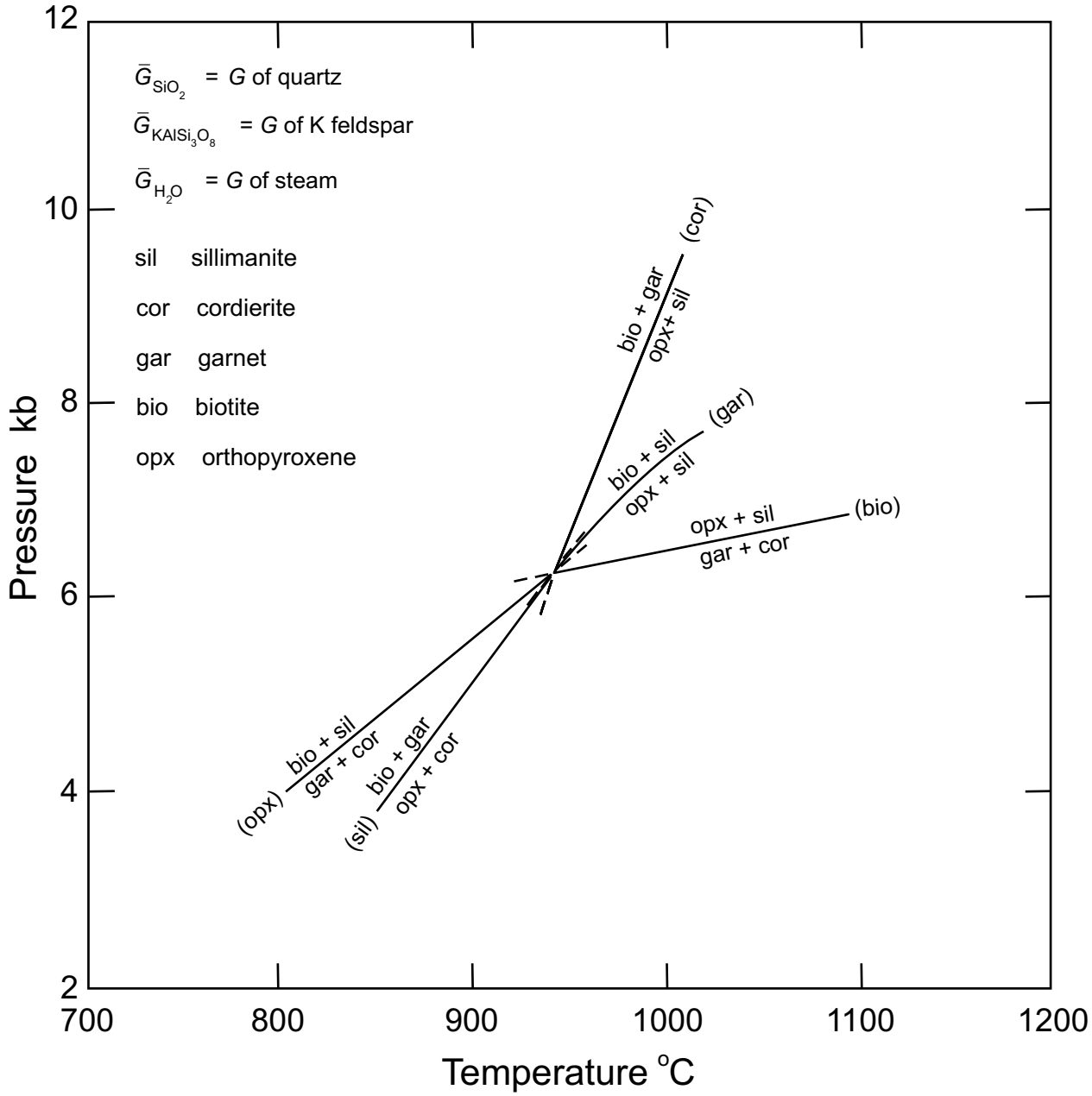

Figure 5. Univariant curves around the invariant point biotite-sillimanite-garnet-cordierite-orthopyroxene in the composition space Al_2O_3 - FeO - MgO - SiO_2 - $KAlSi_3O_8$ - H_2O with Al_2O_3 , FeO, and MgO as *j*-components and SiO_2, $KAlSi_3O_8$, and H_2O as *k*-components.